

Anatomy of a Natural Sunlight Driven CdS/CoTiO₃/ZnO Ternary Photocatalyst for Efficient Optical Properties and Removal of Reactive Orange 30

Divya G.¹, Sakthi D.², Priyadharsan A.², Boobas S.³ and Sivakumar S.^{1*}

1. Department of Chemistry, E.R.K Arts and Science College, Erumiyampatti, Dharmapuri, Tamilnadu – 636905, INDIA

2. Department of Physics, E.R.K Arts and Science College, Erumiyampatti, Dharmapuri, Tamilnadu – 636905, INDIA

3. Department of Physics, Sri Vasavi College, Erode, Tamilnadu – 638316, INDIA

*sivabanu8494@gmail.com

Abstract

ZnO as a promising photocatalyst has gained much attention for the removal of organic pollutants from water. However, the main drawbacks of the relatively low photocatalytic activity and high recombination rate of photoexcited electron-hole pairs restrict its potential applications. Promoting the spatial separation of photoexcited charge carriers is of paramount significance for photocatalysis because the difference in the band positions makes the potential gradient at the composite boundary. In this work, binary CdS/ZnO and CoTiO₃/ZnO are first prepared by dispersion method and then decorated with ZnO particles to construct CdS/CoTiO₃/ZnO ternary composites. For this reason, the CdS/CoTiO₃/ZnO ternary composites was effectively designed and analyzed for the crystalline structure, light absorption, photoexcitation behavior and surface morphological properties by X-ray diffraction, diffuse reflectance UV/visible absorption spectroscopy, photoluminescence spectroscopy and scanning electron micrograph respectively.

The photocatalytic activity was examined by degradation of the dye solution spectrophotometrically. The results of photocatalytic degradation indicated that the CdS/CoTiO₃/ZnO ternary composites are much higher than those of bare CdS, CoTiO₃, ZnO and any binary composites such as CoTiO₃/ZnO and ZnO/CdS. The enhanced activity could be attributed to the drop electron transfer from CdS to ZnO to CoTiO₃ through the interfacial potential gradient in the ternary hybrid conduction bands. The enhanced electron transfer of CdS/CoTiO₃/ZnO ternary composites was also applicable to degrade other reactive dyes.

Keywords: CdS/CoTiO₃/ZnO, Ternary heterojunctions, Reactive Yellow 84, Photocatalytic Efficiency, Natural Sunlight.

Introduction

Dyes are the integral part of our daily life because of beautiful and bright colors but under the major human health

and environment concerns. According to estimated data given by International Bank, around 17–20% water pollution comes from textile industry⁸. Dyes can be categorized as acidic, basic, disperse, azo, anthraquinone depending on their structural moiety. The color content of the dye absorbs sunlight and interferes with the phenomenon of photosynthesis and henceforth inhibited the growth of aquatic life. Therefore, the removal of such toxic reactive dyes in wastewater is a highly essential issue. To remove or degrade the dyes from the contaminated water, many reduction methods including chemical, physical and biological have been employed¹.

With the ever-increasing global energy demand and environmental crisis, exploring and using renewable and clean energy resources have become one of the most important and challenging tasks. Photocatalysis based on semiconductors attracts great attention because of its massive potentials^{3,17} in energy and environmental related fields exemplified by hydrogen/oxygen evolution by water splitting^{9,13,16}, oxidizing organic pollutants^{2,18} and reduction of carbon dioxide^{4,6,25}. The semiconductor absorbs photons with higher energies than its band gap and generates electron-hole pairs that are able to drive the desired reactions. In general, most of the semiconductor photocatalysts consist of one metal center e.g. the well-known TiO₂¹⁵, ZnS²⁶, AgPO₄²² and others^{19,27}.

Semiconductor photocatalysts such as TiO₂ and ZnO can be a green and efficient technology in the field of sewage treatment, because they can effectively dispose many organic pollutants in the sewage compared with other approaches. Additionally, most photocatalytic materials are non-toxic, stable and low-cost^{11,12}. Although ZnO has a lot of advantages such as high quantum efficiency, non-toxic and strong ultraviolet absorption²³, its catalytic efficiency is still unideal.

However, ZnO binary composite materials also have some defects. It cannot selectively photodegrade some hazard pollutants in wastewater, especially halogenated hydrocarbons. Furthermore, the degradation efficiency decreases obviously when there is a variety of pollutants in wastewater.

Recent studies have found that ZnO-based ternary composites have great superiority than binary composites^{10,20}. Besides, they have the function of selective

degradation of some pollutants²¹. Also, it has been found that Ag has a strong adsorption of high carcinogenic halogenated hydrocarbon¹⁴.

In order to enhance the photocatalytic efficiency and stability, it is essential to extend the light absorption range or suppress the recombination of photoexcited electron-hole pairs of ZnO. In recent years, various investigations have been conducted to enhance the photocatalytic efficiency by means of combining the photocatalysts with noble metals, narrow band gap semiconductors, polyaniline, dye sensitization and carbonaceous materials such as carbon nanotubes and C60^{5,7,24,28}.

Taking all these into consideration, we reported herein CdS/CoTiO₃/ZnO ternary composites photocatalysts and investigated its photocatalytic performances. In comparison with the pure ZnO catalyst and CoTiO₃/ZnO binary composite, the ternary CdS/CoTiO₃/ZnO system exhibits much higher photocatalytic activity and excellent cycling performance for removal of reactive yellow 84 in water under solar light irradiation.

Material and Methods

Materials: Titanium tetrachloride (99.5%) supplied by Loba Chemie Pvt. Ltd., ammonia solutions supplied by Merck and cobalt nitrate are used for the preparation of the CoTiO₃ photocatalyst. Zinc chloride (98%) and sodium bicarbonate (99%) were supplied by Merck and used as such for the preparation of the ZnO photocatalyst. Sodium sulfide and cadmium chloride supplied by Merck were used for preparation of CdS. Sodium hydroxide and hydrochloric acid (both AR grades) from Loba Chemie were used as such for adjusting the pH of the dye solutions. Potassium dichromate (AR), silver sulphate (GR), mercury sulphate (GR), 99% ferrous (GR) and sulphuric acid were used for COD analysis. Double distilled deionized water was used for the preparation of dye solutions.

Methods

Synthesis of ZnO photocatalyst: 10 g of zinc chloride was dissolved in 100 mL of double distilled water. To that solution, 6.2 g of sodium bicarbonate was added in portions with vigorous stirring for several minutes. The precipitate formed was washed several times with distilled water to remove NaCl formed. The precipitate was then dried at 100°C to remove the water. The solid obtained after drying was ground in an agate mortar and pressed into a ceramic crucible. The material was calcinated at 500°C for 4 h.

Preparation of Ternary Composite Photocatalysts: In the preparation of 0.5 wt % CoTiO₃/ZnO/CdS ternary composites, 0.05 g of CdS and 0.995 g of CoTiO₃/TiO₂ were mixed with pestle mortar and ground gently to get fine powder. This ternary mixture subsequently annealed at 300°C for 3 h in a Muffle furnace. The CoTiO₃/ZnO/CdS ternary composites with 1, 2, 3 and 4 wt% of CdS were prepared by varying CoTiO₃/ZnO/ and CdS ratios as in a

same method and labeled as CTZC-1, CTZC -2, CTZC -3 and CTZC -4 respectively.

Evaluation of Photocatalytic Activity: The photocatalytic studies were carried out under natural solar light on plain sky atmosphere days during the period of February to May 2019. In a typical experiment, 50 mL of Reactive Yellow 84 solution were taken in 250 mL glass beaker with 50 mg of photocatalyst added and saturated with oxygen by aerating with an air-pump upto 1 h to attain adsorption equilibrium. Then the dye solution (Model pollutant) was set aside in direct sunlight with continuous aeration and the concentration/absorbance of the dye remains was measured in gradual interval time by measuring its light absorbance at the visible λ_{\max} by using an Elico UV-Visible spectrophotometer.

In order to avoid the difference in results due to oscillation in the intensity of the sunlight, a set of experiments have been carried out simultaneously. For pH studies, the pH of the dye solutions was modified to different pH such as 3, 5, 7, 9 and 12 by using 0.1 M HCl and NaOH solution. For concentration studies, the degradation of dye solution of various concentrations at pH 3 was treated using the photocatalyst and the efficiency of the catalyst was calculated from the percentage of degradation of the dye solution.

The percentage of degradation was calculated using the following relation:

$$\% \text{ of Degradation} = \left(\frac{C_0 - C}{C_0} \right) \times 100$$

where C_0 is the initial concentration of the dye solution and C is the concentration of the dye remaining after degradation.

Results and Discussion

X-ray diffraction Analysis: XRD patterns of pure ZnO, CoTiO₃, CdS, 8wt% CoTiO₃/ZnO, 4 wt% CdS/TiO₂ and 1wt % CdS/CoTiO₃/TiO₂ wt % CdS/CoTiO₃/TiO₂ and 5 wt % CdS/CoTiO₃/TiO₂ ternary heterojunction are shown in the figure 3. The diffraction pattern of ZnO exactly matches in JCPDS36-145, which indicates that the ZnO has the hexagonal wurtzite crystal structure. The CoTiO₃ crystal structure exactly matches the JCPDS card no.89-2944 and it has good crystalline phase.

The CdS crystal structure also exactly matches the JCPDS card no.89-2944. The diffraction patterns of CdS/ZnO and CoTiO₃/ZnO heterojunctions are similar like the patterns of wurtzite ZnO. The diffraction peaks of CoTiO₃ and CdS were undetectable in the diffraction patterns of the CdS/ZnO and CoTiO₃/ZnO heterojunction, this could be attributed to the high degree of dispersion of CoTiO₃ and CdS in the matrix of ZnO forming solid solution.

The diffraction patterns of CdS/CoTiO₃/ZnO ternary composites are also similar like the patterns of wurtzite ZnO in the case of lower concentrations of CdS such as 1 and 3 wt%. But, as the CdS weight ratio increases (5wt%), the crystallinity might be decreased. This lower crystallinity indicates CdS cover over the surface of ZnO.

SEM Analysis: Figure 4 illustrates the SEM images of pure CoTiO₃, ZnO and CoTiO₃/ZnO heterojunction and CdS/CoTiO₃/ZnO ternary composites samples. SEM image of pure ZnO are shown in figure 4a providing visualization

of the textural properties of small portions of granules indicating that the pure ZnO is made up of irregularly shaped aggregates. Pure CoTiO₃ SEM image (Fig. 4b) shows small particle size with colloidal surface nature. Figure 4c indicates the micrographs show that CdS particles have blunder particle morphology. Addition of CoTiO₃ has significant effect on the small particle morphology and further increases the level of CoTiO₃ concentration (Fig. 4d and e) up to 8wt%, the particles are highly dispersed and small in particle size.

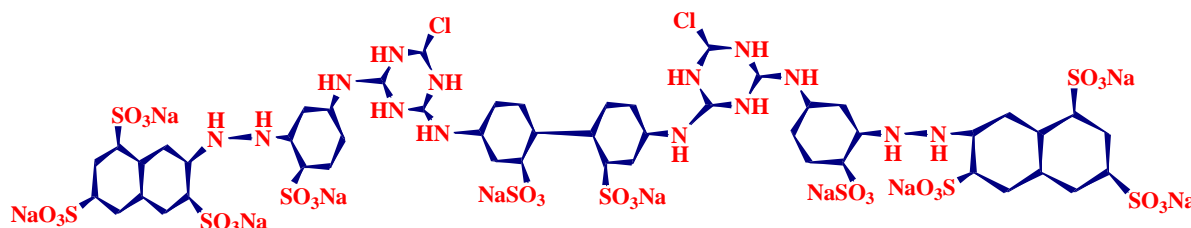


Figure 1: Structure of Reactive Yellow 84

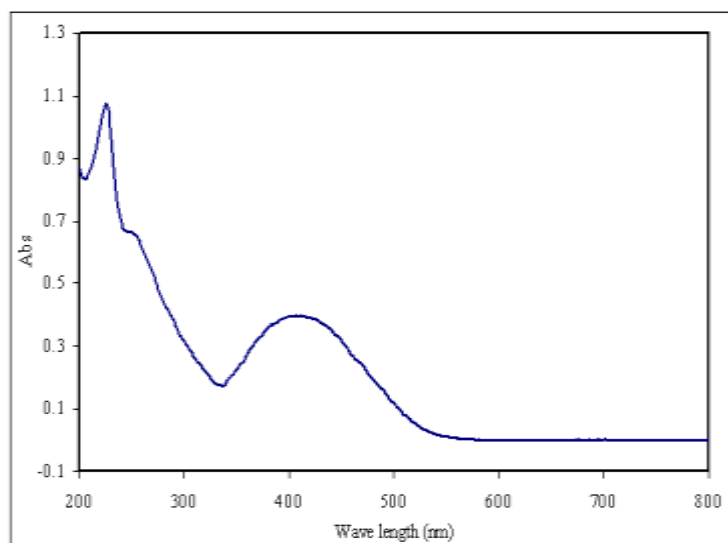


Figure 2: UV-Visible absorbance spectrum of Reactive Yellow 84

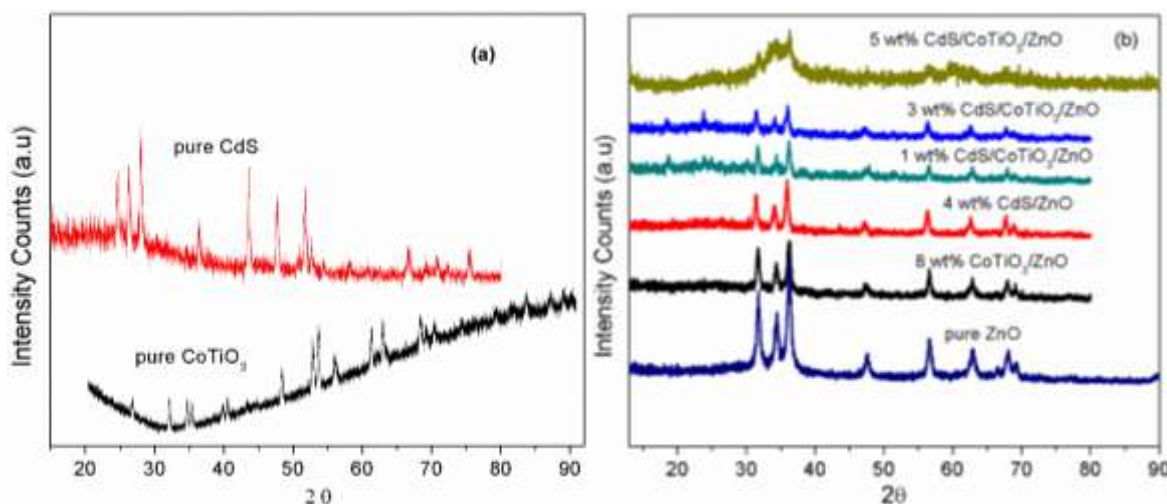


Figure 3: XRD patterns of (a) Pure CoTiO₃, CdS and (b) Pure ZnO, 8 wt% CoTiO₃/TiO₂, 4 wt% CdS/TiO₂ and various concentration of ternary composites

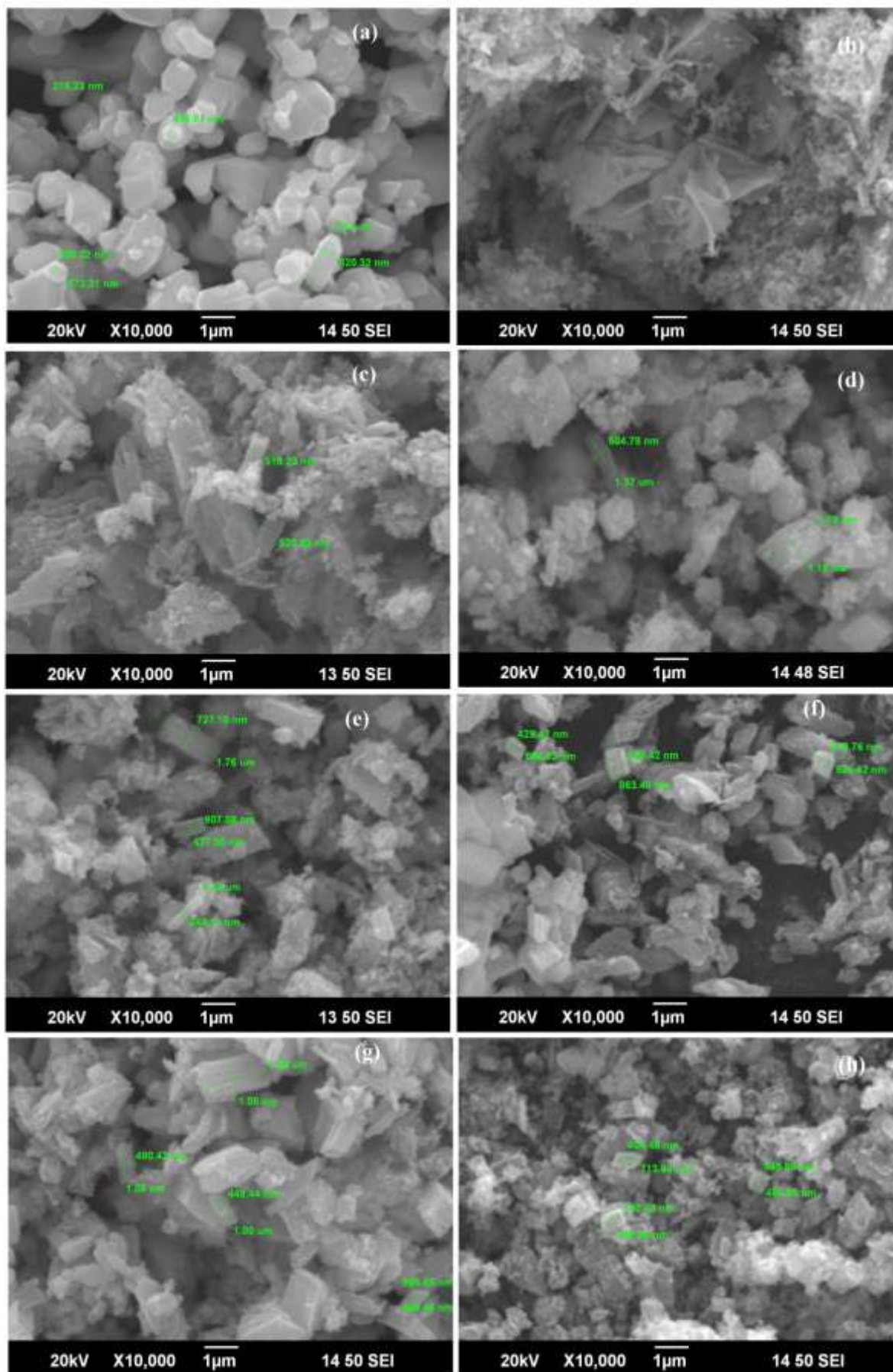


Figure 4: SEM images of Pure ZnO, CoTiO₃, CdS, 8 wt% CoTiO₃/ZnO, 4 wt% CdS/ZnO and various concentration of ternary composites

It is presumed that the concentration of CoTiO_3 as a coupling precursor played a key role in the formation of the peculiar morphology of spheres. After the decoration of CdS particles, the granular materials are observed on the surface of $\text{CoTiO}_3/\text{ZnO}$ (Fig. 4f and 4g) indicating the formation of the $\text{CdS}/\text{CoTiO}_3/\text{ZnO}$ ternary composite.

Further by addition of CdS content to $\text{CoTiO}_3/\text{ZnO}$ binary system, the particles get agglomeration. From this study we find that 4 wt% $\text{CdS}/\text{CoTiO}_3/\text{ZnO}$ ternary composite is suitable for solar light photocatalytic degradation.

DRS Analysis: Optical absorption property of photocatalyst is an important factor in determining the photocatalytic performance since the formation of photogenerated electron-hole pairs and reactive species under light irradiation is the pre-requisite for photocatalytic reaction. The diffuse reflectance spectra of synthesized pure ZnO, CoTiO_3 and CdS, 8 wt% $\text{CoTiO}_3/\text{ZnO}$, 4 wt% CdS/ZnO and various concentrations of ternary composites are displayed in the fig. 5.

The absorption boundary of pure ZnO is at about 400 nm which is consistent with the earlier records. The synthesized ZnO shows absorption only at UV range while the absorption of $\text{CoTiO}_3/\text{ZnO}$ and CdS/ZnO composites shows apparently red-shift and there is improved light absorption in the visible region indicating the coupling CoTiO_3 and CdS on ZnO.

It absorbs more visible light energy than that of binary and parent photocatalyst. This absorbance band position of $\text{CoTiO}_3/\text{CdS}/\text{ZnO}$ composites has been favorable for photocatalytic reaction.

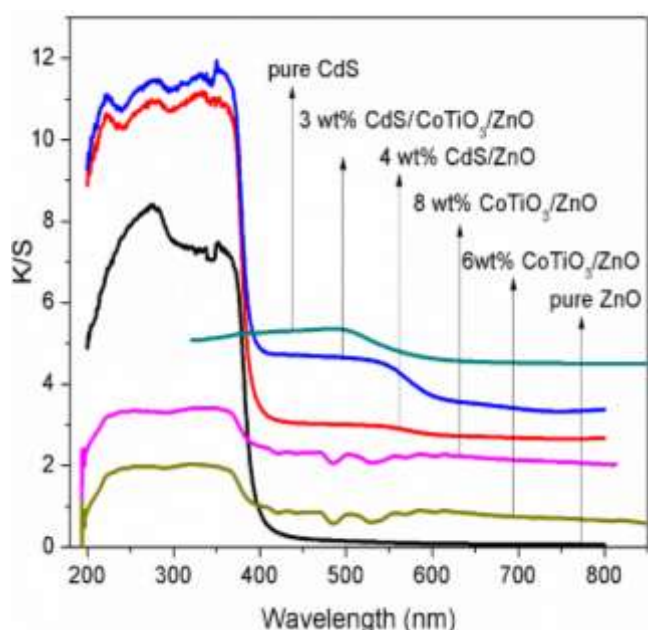


Figure 5: UV-visible diffused reflectance spectra of pure ZnO, CoTiO_3 , CdS, 6 wt% $\text{CoTiO}_3/\text{ZnO}$, 8 wt% $\text{CoTiO}_3/\text{ZnO}$, 4 wt% CdS/ZnO and various concentrations of ternary composites

Photoluminescence Study: Efficiency of charge carrier trapping, migration and transfer in a photocatalytic material help to understand the nature of electron-hole pairs in photocatalyst. Excited electrons in the conduction band recombine with photogenerated holes generated in the valence band accompanying with PL emission.

Figure 4 shows the PL spectra of pure ZnO, 8 wt% $\text{CoTiO}_3/\text{ZnO}$, 4 wt% CdS/ZnO and 3 wt% $\text{CoTiO}_3/\text{CdS}/\text{ZnO}$ ternary composites recorded by exciting the material at 360 nm. The PL spectrum of both photocatalysts has an emission peak at 628 nm.

However, the intensity of the emission in $\text{CoTiO}_3/\text{CdS}/\text{ZnO}$ ternary composites is much smaller than that of binary and parent photocatalysts. The lower PL intensity of $\text{CoTiO}_3/\text{CdS}/\text{ZnO}$ ternary composites indicates the electron-hole pair recombination in ternary composites reduced by charge separation between two semiconductors.

Photocatalytic activity: There is only a tiny portion (4%) of solar radiation in the UV region, while visible light is far more abundant (46%), thus enhancing the photocatalytic capability of semiconductors under visible light as well as UV light irradiation which has become a necessary issue in order to highly utilize solar energy.

To study the photocatalytic degradation efficiency of the $\text{CdS}/\text{CoTiO}_3/\text{ZnO}$ ternary photocatalytic system, the photocatalytic activities of various photocatalysts materials are evaluated for the degradation of RY 84 solution as a model dye effluent under irradiation with solar light. Dark adsorption of dye molecules is measured for 20 min to reach an adsorption-desorption equilibrium.

In this work, RY 84, with a characteristic absorption at 410 nm, is chosen as a typical dye pollutant for testing the photocatalytic activity of the as-prepared products under both UV and visible light irradiation.

Figure 7(a) shows the instantaneous RY 84 concentrations variations versus time in the presence of ternary composites, binary system as well as parent photocatalyst under solar light irradiation, respectively. The graphs in the first 20 min before light irradiation are caused by the RY 84 adsorption-desorption process on the catalyst surfaces.

It can be seen that only 4% decrease in the concentration of RY 84 can be observed in the presence of ZnO as the adsorption-desorption equilibrium of RY 84 on the surface of ZnO photocatalyst reaches in dark after 20 min ultrasonic treatment.

The adsorption ability of RY 84 over CdS, CoTiO_3 , CdS/ZnO , $\text{CoTiO}_3/\text{ZnO}$ and $\text{CdS}/\text{CoTiO}_3/\text{ZnO}$ ternary system is up to increase of 20% respectively which may be attributed to the smaller particle size with high specific surface area.

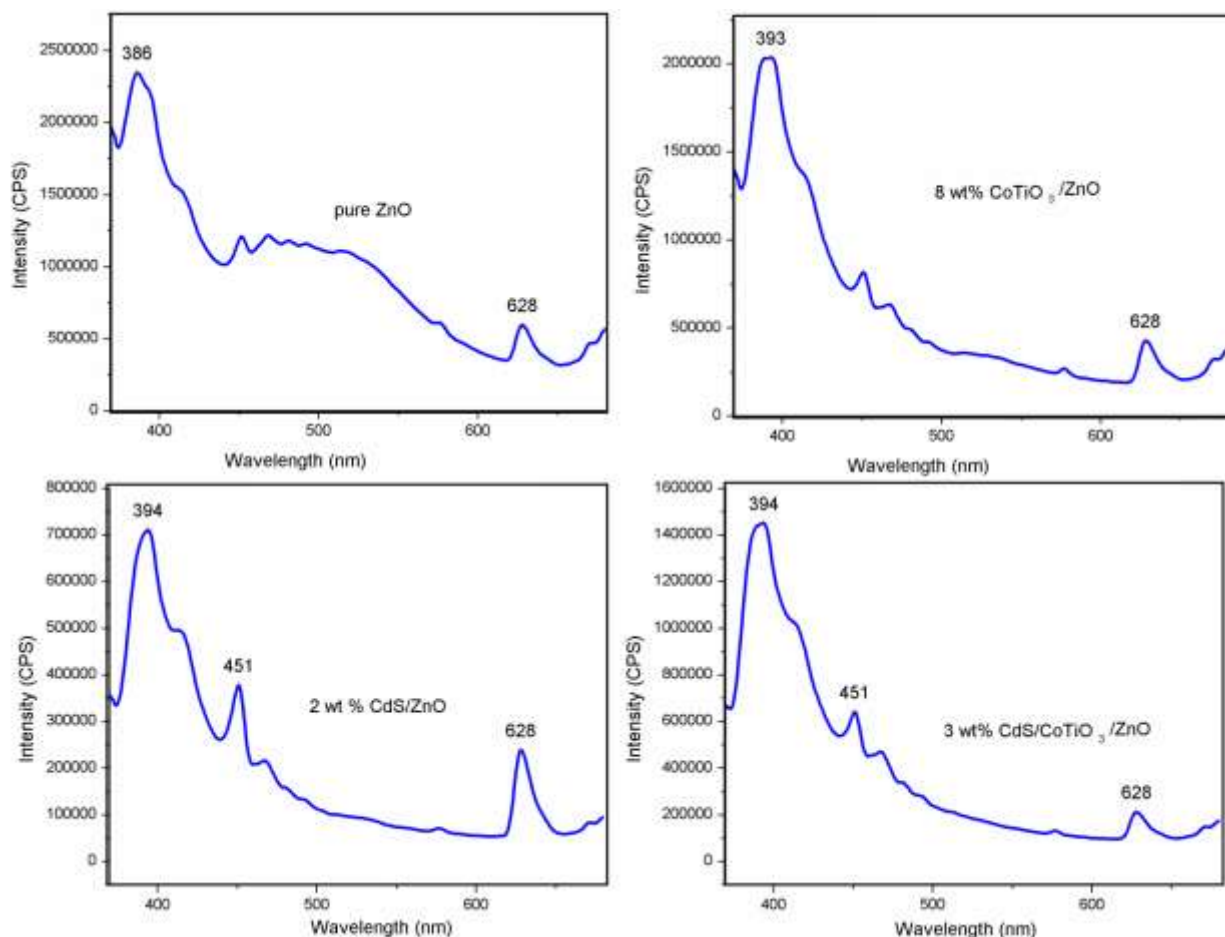


Figure 6: Photoluminescence spectra of photocatalysts

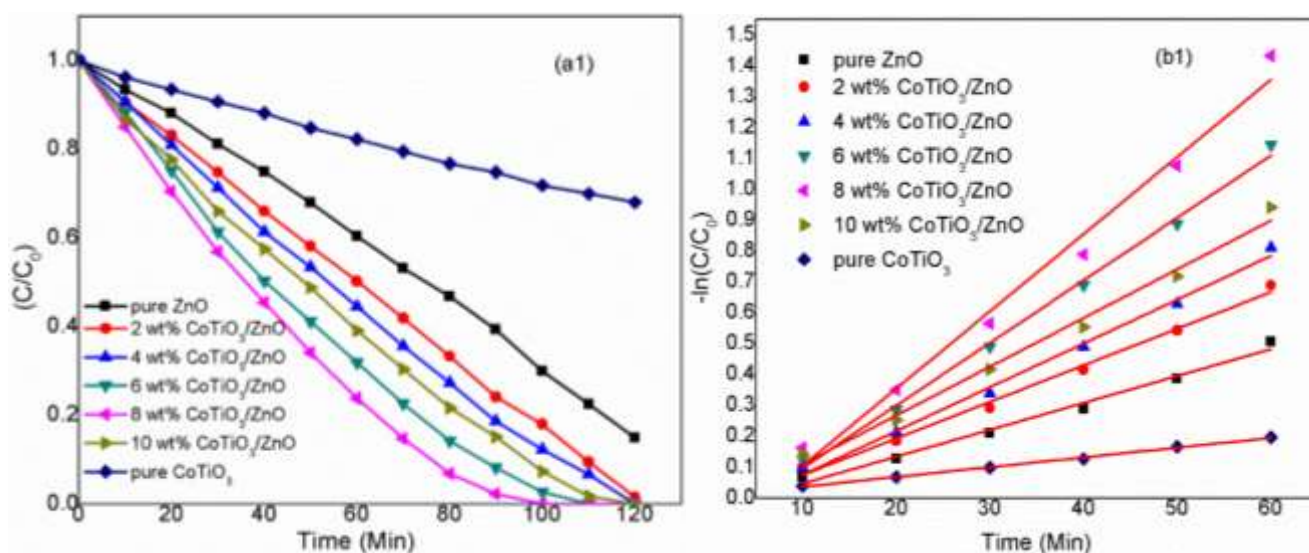


Figure 7a and b: Kinetics of degradation of Reactive Yellow 84 over ZnO, various CoTiO₃/ZnO heterojunction semiconductors, (initial concentration C₀ = 50 mg l⁻¹)

The optimized CoTiO₃/ZnO heterojunction semiconductor further tested the photocatalytic degradation ability when modified with various concentration of CdS with CoTiO₃/ZnO under the same protocol. Fig. 8a exhibits the photocatalytic activities of the CdS/CoTiO₃/ZnO ternary composite semiconductors in the presence of solar light irradiations. After 60 min of UV-visible (solar) illumination,

the RY 84 degrades over CdS and CoTiO₃/ZnO heterojunction semiconductor as only 28% and 78%, respectively. However, CdS/CoTiO₃/ZnO ternary composite semiconductors show higher photocatalytic degradation rate (80–98%) in the presence of same experimental conditions. It is worth noting that CdS coated CoTiO₃/ZnO ternary semiconductor could be inducing notable photodegradation

efficiency from 80% to 98% beyond the increases of 4 wt % of CdS.

From the results, the photocatalytic activity of CoTiO₃/ZnO heterojunction systems increases with the increase in CdS content 1wt % to 4 wt % due to the tightly bonded or close contact interfaces between binary CoTiO₃/ZnO semiconductors. On the contrary, when the mass ratio was higher than 4 wt%, the CdS got agglomerated and it was not well dispersed. This hinders the smooth contact between CoTiO₃/ZnO heterojunction systems and CdS leading to a negative influence on the activity of the 5 wt% CdS/CoTiO₃/ZnO ternary composite.

The studies also show that photoelectron injector such as CdS has very low photocatalytic activity in UV-visible light when compared to that of CoTiO₃/ZnO heterojunction systems. This shows that the CdS has a smaller electron-hole diffusion length than the CoTiO₃/ZnO heterojunction systems and ZnO.

The data obtained from the degradation studies were analysed with the Langmuir–Hinshelwood kinetic model:

$$r_s = \frac{kKc}{1 + Kc}$$

where r_s is the specific degradation reaction rate of the dye ($\text{mg l}^{-1} \text{min}^{-1}$), C is the concentration of the dye (mg l^{-1}), k the reaction rate constant (min^{-1}) and K is the dye adsorption constant. When the concentration (C) is small enough, the above equation can be simplified in an apparent first-order equation:

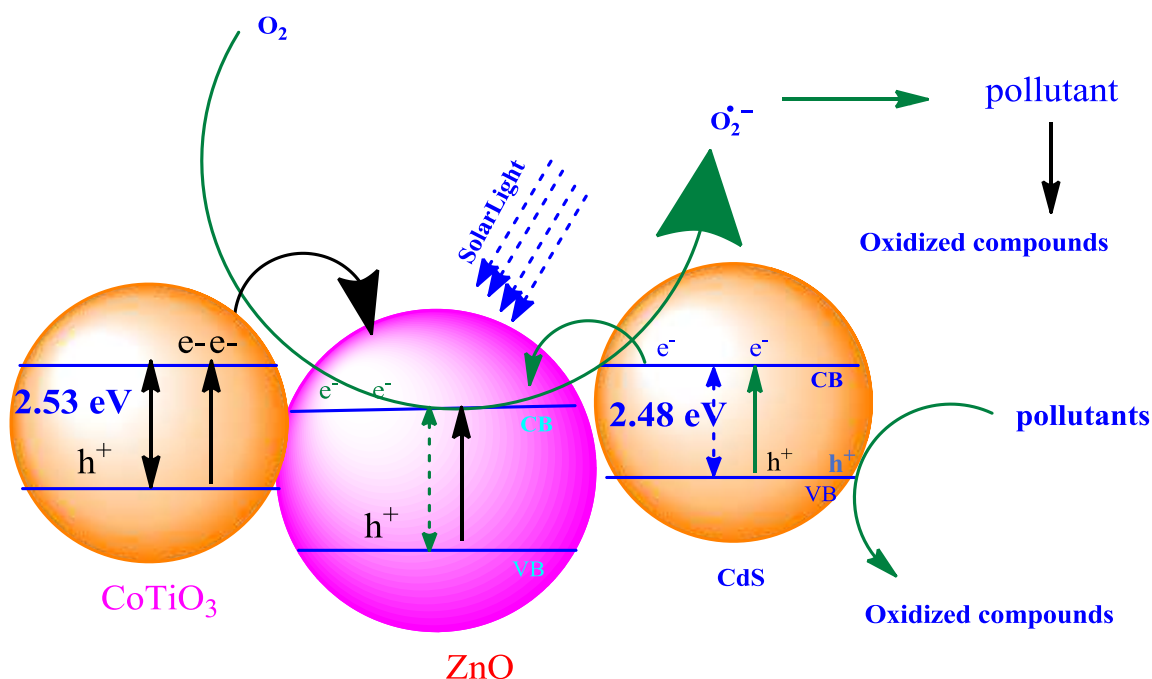
$$r_s = kKc = K_{app} C \left(= -\frac{dc}{dt} \right)$$

After integration, we will get

$$-\ln \left(\frac{C}{C_0} \right) = k_{app} t$$

where C_0 is the initial concentration (mg L^{-1}), C is the concentration of the dye after (t) minutes of illumination. The data obtained from the degradation of RY-84 fits well for the apparent first order kinetics (Fig. 7b and fig. 8b). The electrons in the conduction band can be transferred to surface adsorbed oxygen molecules and form superoxide anions, which can further transform to OH^{\bullet} and initiate the degradation of RY 84.

Photocatalytic Mechanism: We proposed a mechanism for the degradation of reactive yellow 84 on CdS/CoTiO₃/ZnO ternary composites under solar light irradiation as shown in scheme 1. The electron injection from CdS, CoTiO₃ to ZnO semiconductor was investigated. The excited electrons from the CdS particle are quickly transferred to ZnO since the conduction band of CdS show more negative potential than that of ZnO. CdS coupled ZnO system has a beneficial role in improving feeding of electron and extends ZnO in response to visible light. CdS/ZnO can be coupled by electron transfer from irradiated CdS to its conduction band. The electrons are then scavenged by molecular oxygen O_2 to yield the superoxide radical anion $\text{O}_2^{\bullet-}$. These new formed intermediates can interact to produce hydroxyl radical OH^{\bullet} . It might be that the OH^{\bullet} radical is a powerful oxidizing agent capable of degrading most pollutants.



Scheme 1: Photoelectron injection mechanism proposed on CdS/CoTiO₃/ZnO ternary composites

However, the photo-generated holes in CdS cannot oxidize hydroxyl groups to hydroxyl radicals due to its valence band potential. This results in photocorrosion of CdS forming cadmium cations. An approach is still pursued to make the CdS photocatalyst stable, so that this imbalance activity will be managed by CoTiO₃ coupled with CdS/ZnO binary composites. As shown in scheme, in the combination of CoTiO₃ and CdS/ZnO binary composites, the photocurrent is produced by transferring e⁻ from CoTiO₃ to the CdS/ZnO when exposed to UV-visible light. This process can also prevent the e⁻ and H⁺ from recombination. Finally, it is worthy of pointing out that the transformation electron from CoTiO₃ is possible by photo-oxidizing which make the CoTiO₃ in system un-losing. Thus, the CdS/CoTiO₃/ZnO

ternary composite system is a hopeful form for further improving the practicability of CoTiO₃ to the CdS/ZnO.

Reusability of CdS/CoTiO₃/ZnO ternary composite: Moreover the enhanced photocatalytic activity, another significant issue for the practical application of ternary composite photocatalyst is its stability and reusability. In view of this point, three consecutive photodegradation cycles for RY 84 over CdS/CoTiO₃/ZnO ternary composite under solar light are performed by collecting and reusing the CdS/CoTiO₃/ZnO ternary composite. After each photocatalytic run, the CdS/CoTiO₃/ZnO ternary composite is centrifuged and washed several times. Figure 9 illustrates the photocatalytic stability measurement of CdS/CoTiO₃/ZnO ternary composite.

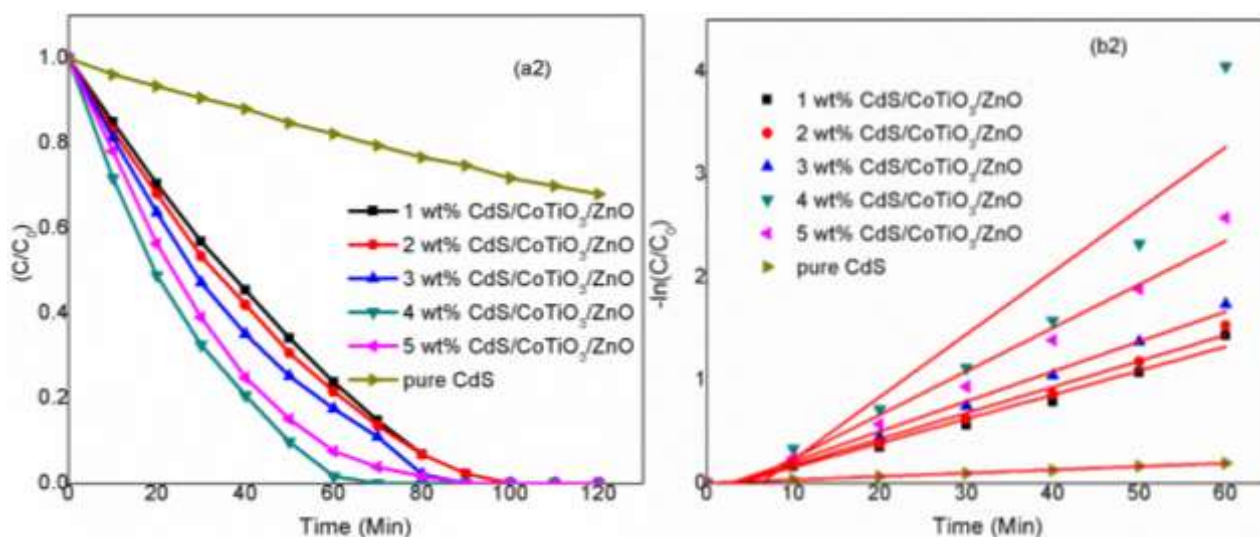


Figure 8a and b: Kinetics of degradation of Reactive Yellow 84 over CdS and CdS/CoTiO₃/ZnO ternary composites (initial concentration $C_0 = 50 \text{ mg l}^{-1}$)

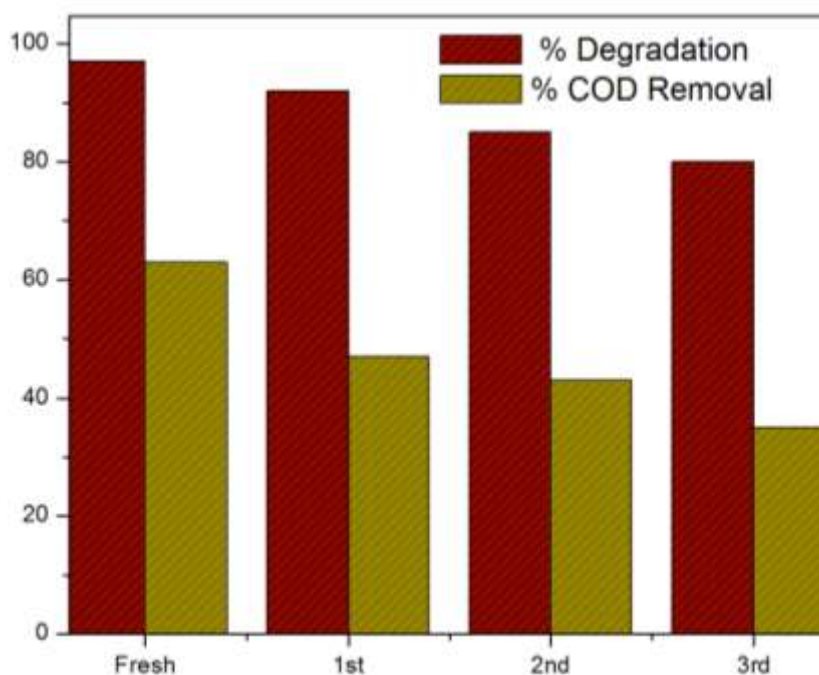


Figure 9: Reusability of 4 wt% CdS/CoTiO₃/ZnO ternary composite

It can be seen that no noticeable loss of the photocatalytic activity has been detected after third repetitious runs, confirming that the structurally designed CdS/CoTiO₃/ZnO ternary composite is quite stable for the photodegradation of organic contaminants. The percentage of the photo mineralization of 50 mg/l Reactive Yellow 84 solution in the third cycle 89% and the COD reduction was 45% in two hours of solar light irradiation. The gradual decrease in the photocatalytic activity after each cycle may be due to the accumulation of intermediates formed during the degradation of dye.

Conclusion

The present investigation involves the development of new methods for the efficient and cost-effective treatment of textile effluents. The familiar photocatalysts like ZnO show better photocatalytic efficiency when coupled with narrow band semiconductors than that of other surface modifications techniques. Hence, in this view, heterojunction composites such as CdS/ZnO and CoTiO₃/ZnO were prepared in a simple dispersed method from the metal oxides synthesized from sol-gel method. The heterojunction composites have been evaluated from their activity in the degradation of Reactive Yellow 84 in the presence of solar light.

From the degradation result, CdS/CoTiO₃/ZnO ternary composites showed higher photocatalytic activity than that of CdS/ZnO and CoTiO₃/ZnO binary heterojunctions shows the favorable photocatalytic activity at pH = 5. The mineralization of reactive dyes with triazine groups has been reported to be more difficult in most treatment methods. But CdS/CoTiO₃/ZnO ternary composites are highly suitable for above mentioned triazine grouped dyes.

References

1. Chakrabarti S. and Dutta B.K., Photocatalytic degradation of model textile dyes in wastewater using ZnO as semiconductor catalyst, *J. Hazard Mater.*, **112(3)**, 269–278 (2004)
2. Chen C., Ma W. and Zhao J., Semiconductor-mediated photodegradation of pollutants under visible-light irradiation, *Chem. Soc. Rev.*, **39(11)**, 4206–4219 (2010)
3. Chung I., Lee B., He J., Chang R.P.H. and Kanatzidis M.G., All-solid-state dye-sensitized solar cells with high efficiency, *Nature*, **485(7399)**, 486–489 (2012)
4. Dhakshinamoorthy A., Navalon S., Corma A. and Garcia H., Photocatalytic CO₂ reduction by TiO₂ and related titanium containing solids, *Energy Environ. Sci.*, **5(11)**, 9217–9233 (2012)
5. Eskizeybek V., Sari F., Gülce H., Gülce A. and Avci A., Preparation of the new polyaniline/ZnO nanocomposite and its photocatalytic activity for degradation of methylene blue and malachite green dyes under UV and natural sun lights irradiations, *Appl. Catal. B Environ.*, **119–120**, 197–206 (2012)
6. He Y., Wang Y., Zhang L., Teng B. and Fan M., High-efficiency conversion of CO₂ to fuel over ZnO/g-C₃N₄ photocatalyst, *Appl. Catal. B Environ.*, **168–169**, 1–8 (2015)
7. Jana T.K., Pal A. and Chatterjee K., Self assembled flower like CdS-ZnO nanocomposite and its photo catalytic activity, *J. Alloys Compd.*, **583**, 510–515 (2014)
8. Kant R., Textile dyeing industry an environmental hazard, *Nat. Sci.*, **04(01)**, 22–26 (2012)
9. Lang J., Liu M., Su Y., Yan L. and Wang X., Fabrication of the heterostructured CsTaWO₆/Au/g-C₃N₄ hybrid photocatalyst with enhanced performance of photocatalytic hydrogen production from water, *Appl. Surf. Sci.*, **358**, 252–260 (2015)
10. Lan M., Fan G., Yang L. and Li F., Enhanced visible-light-induced photocatalytic performance of a novel ternary semiconductor coupling system based on hybrid Zn-In mixed metal oxide/g-C₃N₄ composites, *RSC Adv.*, **5(8)**, 5725–5734 (2015)
11. Lehmann J. and Kleber M., The contentious nature of soil organic matter, *Nature*, **528(7580)**, 60–68 (2015)
12. Lei J.F., Li L.B., Shen X.H., Du K., Ni J., Liu C.J. and Li W.S., Fabrication of ordered ZnO/TiO₂ heterostructures via a templating technique, *Langmuir*, **29(45)**, 13975–13981 (2013)
13. Li X., Yu J., Low J., Fang Y., Xiao J. and Chen X., Engineering heterogeneous semiconductors for solar water splitting, *J. Mater. Chem. A*, **3(6)**, 2485–2534 (2015)
14. Liu H.R., Shao G.X., Zhao J.F., Zhang Z.X., Zhang Y., Liang J., Liu X.G., Jia H.S. and Xu B.S., Worm-like Ag/ZnO core-shell heterostructural composites: Fabrication, characterization and photocatalysis, *J. Phys. Chem. C*, **116(30)**, 16182–16190 (2012)
15. Perera S.D., Mariano R.G., Vu K., Nour N., Seitz O., Chabal Y. and Balkus K.J., Hydrothermal Synthesis of Graphene-TiO₂ Nanotube Composites with Enhanced Photocatalytic Activity, *ACS Catal.*, **2(6)**, 949–956 (2012)
16. Reece S.Y., Hamel J.A., Sung K., Jarvi T.D., Esswein A.J., Pijpers J.J.H. and Nocera D.G., Wireless solar water splitting using silicon-based semiconductors and earth-abundant catalysts, *Science*, **334(6056)**, 645–648 (2011)
17. Schrauben J.N., Hayoun R., Valdez C.N., Braten M., Fridley L. and Mayer J.M., Titanium and zinc oxide nanoparticles are proton-coupled electron transfer agents, *Science*, **336(6086)**, 1298–1301 (2012)
18. Wang Y., Shi R., Lin J. and Zhu Y., Enhancement of photocurrent and photocatalytic activity of ZnO hybridized with graphite-like C₃N₄, *Energy Environ. Sci.*, **4(8)**, 2922–2929 (2011)
19. Wetchakun N., Chaiwichain S., Inceesungvorn B., Pingmuang K., Phanichphant S., Minett A.I. and Chen J., BiVO₄/CeO₂ Nanocomposites with High Visible-Light-Induced Photocatalytic Activity, *ACS Appl. Mater. Interfaces.*, **4(7)**, 3718–3723 (2012)
20. Wu J.G., Fang T., Cai R., Li S.Y., Wang Y., Zhao C.E. and Wei A., Fabrication of an Ag/Fe₂O₃/ZnO ternary composite with enhanced photocatalytic performance, *RSC Adv.*, **6(5)**, 4145–4150 (2016)

21. Xue J., Ma S., Zhou Y., Zhang Z. and Jiang P., Synthesis of Ag/ZnO/C plasmonic photocatalyst with enhanced adsorption capacity and photocatalytic activity to antibiotics, *RSC Adv.*, **5(24)**, 18832–18840 (2015)
22. Yang Z.M., Huang G.F., Huang W.Q., Wei J.M., Yan X.G., Liu Y.Y., Jiao C., Wan Z. and Pan A., Novel Ag₃PO₄/CeO₂ composite with high efficiency and stability for photocatalytic applications, *J. Mater. Chem. A.*, **2(6)**, 1750–1756 (2014)
23. Yin B., Qiu Y., Zhang H., Lei J., Chang Y., Ji J., Luo Y., Zhao Y. and Hu L., Piezoelectric effect of 3-D ZnO nanotetrapods, *RSC Adv.*, **5(15)**, 11469–11474 (2015)
24. Yin X., Que W., Fei D., Shen F. and Guo Q., Ag nanoparticle/ZnO nanorods nanocomposites derived by a seed-mediated method and their photocatalytic properties, *J. Alloys Compd.*, **524**, 13–21 (2012)
25. Yu W., Xu D. and Peng T., Enhanced photocatalytic activity of g-C₃N₄ for selective CO₂ reduction to CH₃OH via facile coupling of ZnO: A direct Z-scheme mechanism, *J. Mater. Chem. A*, **3(39)**, 19936–19947 (2015)
26. Yu Y.X., Ouyang W.X., Liao Z.T., Du B.B. and Zhang W.D., Construction of ZnO/ZnS/CdS/CuInS₂ Core–Shell Nanowire Arrays via Ion Exchange: p–n Junction Photoanode with Enhanced Photoelectrochemical Activity under Visible Light, *ACS Appl. Mater. Interfaces*, **6(11)**, 8467–8474 (2014)
27. Yuan Y., Huang G.F., Hu W.Y., Xiong D.N., Zhou B.X., Chang S. and Huang W.Q., Construction of g-C₃N₄/CeO₂/ZnO ternary photocatalysts with enhanced photocatalytic performance, *J. Phys. Chem. Solids*, **106**, 1–9 (2017)
28. Zhang Q., Dandeneau C.S., Zhou X. and Cao G., ZnO Nanostructures for Dye-Sensitized Solar Cells, *Adv. Mater.*, **21(41)**, 4087–4108 (2009).

(Received 11th October 2020, accepted 22nd December 2020)